VgrG C terminus confers the type VI effector transport specificity and is required for binding with PAAR and adaptor–effector complex

Devanand D. Bondage[a,b,c], Jer-Sheng Lin[a], Lay-Sun Ma[a], Chih-Horng Kuo[a,b,d], and Erh-Min Lai[a,b,d,1]

[a]Institute of Plant and Microbial Biology, Academia Sinica, Taipei 11529, Taiwan; [b]Molecular and Biological Agricultural Sciences Program, Taiwan International Graduate Program, Academia Sinica, Taipei 11529, Taiwan; [c]Graduate Institute of Biotechnology, National Chung-Hsing University, Taichung 40227, Taiwan; and [d]Biotechnology Center, National Chung-Hsing University, Taichung 40227, Taiwan

Edited by John J. Mekalanos, Harvard Medical School, Boston, MA, and approved May 17, 2016 (received for review January 13, 2016)

Type VI secretion system (T6SS) is a macromolecular machine used by many Gram-negative bacteria to inject effectors/toxins into eukaryotic hosts or prokaryotic competitors for survival and fitness. To date, our knowledge of the molecular determinants and mechanisms underlying the transport of these effectors remains limited. Here, we report that two T6SS encoded valine-glycine repeat protein G (VgrG) paralogs in *Agrobacterium tumefaciens* C58 specifically control the secretion and interbacterial competition activity of the type VI DNase toxins Tde1 and Tde2. Deletion and domain-swapping analysis identified that the C-terminal extension of VgrG1 specifically confers Tde1 secretion and Tde1-dependent interbacterial competition activity *in planta*, and the C-terminal variable region of VgrG2 governs this specificity for Tde2. Functional studies of VgrG1 and VgrG2 variants with stepwise deletion of the C terminus revealed that the C-terminal 31 aa (C31) of VgrG1 and 8 aa (C8) of VgrG2 are the molecular determinants specifically required for delivery of each cognate Tde toxin. Further in-depth studies on Tde toxin delivery mechanisms revealed that VgrG1 interacts with the adaptor/chaperone–effector complex (Tap-1–Tde1) in the absence of proline-alanine-alanine-arginine (PAAR) and the VgrG1–PAAR complex forms independent of Tap-1 and Tde1. Importantly, we identified the regions involved in these interactions. Although the entire C31 segment is required for binding with the Tap-1–Tde1 complex, only the first 15 aa of this region are necessary for PAAR binding. These results suggest that the VgrG1 C terminus interacts sequentially or simultaneously with the Tap-1–Tde1 complex and PAAR to govern Tde1 translocation across bacterial membranes and delivery into target cells for antibacterial activity.

type VI secretion system | VgrG | DNase effector | interbacterial competition | *Agrobacterium tumefaciens*

The type VI secretion system (T6SS) is a molecular weapon used by many Gram-negative bacteria to inject effectors into eukaryotic host cells or competing prokaryotes for various functions. A number of T6SS-secreted effectors were recently found to have contact-dependent antibacterial activity in various bacteria (1). The biochemical functions of characterized effectors include the cell wall-degrading enzymes (2–5), nuclease (6–8), and membrane lipid-degrading phospholipase (9–11). These diverse toxin effectors are widespread superfamilies in the bacterial kingdom and therefore likely have a general antibacterial strategy against competitor bacterial cells. Moreover, some bacterial toxins, such as cell wall-degrading lysozyme or amidase, may function beyond a weapon used by eubacteria because some archaea and eukaryotes have acquired these genes to defend against the bacterial attackers (12, 13).

Functional and structural studies have shown that the T6SS nanomachine shares striking similarities with the bacteriophage tail structure (14–22). Accumulating evidence suggests that the baseplate complex is recruited into the membrane-associated protein complex and initiates the polymerization of a TssB-TssC (VipA-VipB) contractile sheath. The TssB-TssC sheath wraps around the Hcp (hemolycin-coregulated protein)-VgrG (valine-glycine repeat protein G) tail tube/puncturing device and dynamically propels Hcp-VgrG and type VI effectors across bacterial membranes. As a result, Hcp and VgrG are released into the extracellular milieu. In addition to its assembly into homohexameric hollow ring structures, Hcp can function as a chaperone and receptor for certain effectors bound to its inner cavity for transport across double membranes (23). Some unusually large Hcp proteins harboring putative catalytic domains, and therefore possibly having effector functions, have yet to be characterized (24).

VgrG protein is involved in recognition and transport of a specific set of effectors as well. It may feature the effector function at the C-terminal domain. Such "evolved VgrGs" include *Vibrio cholerae* VgrG-1, with an actin cross-linking domain; *Aeromonas hydrophila* VgrG1, with an actin-ADP ribosylating VIP-2 domain; and *V. cholerae* VgrG-3, with glycoside hydrolase activity to target peptidoglycan (9, 25–27). Furthermore, VgrG may function as a carrier for effector delivery by binding directly with specific effectors carrying the proline-alanine-alanine-arginine (PAAR) domain (28, 29).

Thus, Hcp and VgrG each seem to be a vehicle for specific effector secretion across bacterial membranes. Importantly, genes encoding known or putative effectors are often found adjacent to or near *vgrG* (1, 6, 7, 10) and the requirement of the cognate *vgrG* for specific type VI toxin-mediated interbacterial competition was demonstrated in *Pseudomonas aeruginosa* and *Enterobacter cloacae*

Significance

The type VI secretion system involves multiple strategies for effector delivery via fusion or interaction of effectors to structural components of the phage tail-like structure, the tube component Hcp or spike protein VgrG. However, the detailed mechanisms underlying how diverse VgrG proteins govern effector delivery remains unclear. Here, we report that the divergent C-terminus of VgrG protein is the molecular determinant governing specific effector delivery and is required for interacting with a specific adaptor/chaperone protein that stabilizes and binds directly with the cognate effector. The striking conservation of genetic modules encoding homologous VgrG, a distinct set of potential adaptor/chaperone, and a specific effector in various Proteobacteria strongly suggest a conserved mechanism in type VI effector delivery.

Author contributions: D.D.B. and E.-M.L. designed research; D.D.B. and J.-S.L. performed research; D.D.B., J.-S.L., L.-S.M., and C.-H.K. contributed new reagents/analytic tools; D.D.B., C.-H.K., and E.-M.L. analyzed data; and D.D.B. and E.-M.L. wrote the paper.

The authors declare no conflict of interest.

This article is a PNAS Direct Submission.

Freely available online through the PNAS open access option.

[1]To whom correspondence should be addressed. Email: emlai@gate.sinica.edu.tw.

This article contains supporting information online at www.pnas.org/lookup/suppl/doi:10.1073/pnas.1600428113/-/DCSupplemental.

(30, 31). Recent studies further identified a DUF4123–domain-containing protein, Tap-1/Tec, that is required for loading a specific effector onto cognate VgrG for delivery in *V. cholerae* (32, 33). Interestingly, the C terminus of VgrG in *Escherichia coli* Sci-1 T6SS interacts directly with the Tle1 phospholipase effector for delivery without bridging by an adaptor protein (11). However, the detailed molecular determinants and underlying mechanisms of VgrG-conferred effector transport specificity have not been elucidated.

Agrobacterium tumefaciens C58 harbors one T6SS that is activated transcriptionally by an ExoR-ChvG/ChvI signaling cascade and posttranslationally via threonine phosphorylation when sensing acidity (34–36). Three type VI effectors, namely type VI amidase effector (Tae) and type VI DNase effectors (Tde1 and Tde2), confer antibacterial activity of this bacterium. Autointoxication is prevented through the production of cognate immunity proteins (namely Tai, Tdi1, and Tdi2) (6). Both Tde DNase toxins harbor a C-terminal toxin_43 domain and confer interbacterial competition activity during plant colonization (6). In silico analysis further revealed a well-conserved genetic linkage of the *tde-tdi* gene pair with *vgrG* in many T6SS-encoding Proteobacteria (6).

Here, we investigated whether Tde secretion and Tde-dependent antibacterial activity depend on genetically linked genes encoding cognate VgrG and known or putative adaptor/chaperones. We established that the C-terminal variable/extension region of VgrG is the specific molecular determinant conferring Tde toxin delivery and is required for binding to a PAAR protein and a cognate adaptor/chaperone that interacts directly with a specific effector. Furthermore, protein–protein interactions in various mutants led to a proposed model in which the Tde effector is stabilized and carried by its cognate adaptor/chaperone, which loads the effector onto the C terminus of VgrG for secretion across bacterial membranes.

Results

In Silico Analysis of *A. tumefaciens* VgrG Proteins. *A. tumefaciens* strain C58 encodes two VgrG proteins, VgrG1 and VgrG2, which are functionally redundant in mediating secretion of the hallmark T6SS protein Hcp (37). However, the exact role of each VgrG protein in the function of *A. tumefaciens* T6SS remains elusive. VgrG1 and VgrG2 contain 816- and 754-aa residues, respectively, and share ∼92% amino acid identity, with high sequence variations at the C-terminal end (Fig. S1). Domain prediction with the Phyre2 protein fold-recognition server (38) revealed the presence of the domains gp27 (18–370 aa in both VgrG1 and VgrG2) and gp5 (380–757 aa in VgrG1 and 380–754 aa in VgrG2) (Figs. S1 and S2*A*). No recognizable effector domain was identified in the C-terminal region of VgrG1 or VgrG2 by sequence similarity based on a National Center for Biotechnology Information (NCBI) CD-search (39) or structure similarity based on Phyre2 analysis, which suggests that *A. tumefaciens* VgrG proteins belong to the group of "canonical VgrG" proteins. Furthermore, the 3D structure predicted by homology modeling showed that *A. tumefaciens* VgrG1 resembles the monomeric gp27–gp5 protein complex structure, except for the lysozyme domain (Fig. S2*B*). Thus, we considered *A. tumefaciens* VgrG1 and VgrG2 as structural homologs of the gp27–gp5 protein complex that constitutes the cell-puncturing apparatus of T4 bacteriophage.

VgrG1 Is Specifically Required for Tde1 Secretion and Tde1-Dependent Interbacterial Competition Activity *in Planta*. In view of the genetic linkage of *vgrG1* to the *tde1-tdi1* pair residing in the major T6SS gene cluster and *vgrG2* to *tde2-tdi2* encoded in a divergent *vgrG2* operon (Fig. 1*A*), we hypothesized that VgrG1 and VgrG2 are specific carriers for secretion and delivery of Tde1 and Tde2, respectively, into target cells. To test this theory, we first performed secretion assays of each *vgrG* single- and double-deletion mutant strain. The Δ*vgrG1* or Δ*vgrG2* strain remained fully functional in secretion of Hcp and Tae toxin; however, the secretion of Tde1 toxin was no longer detectable in Δ*vgrG1* but remained normal in Δ*vgrG2*

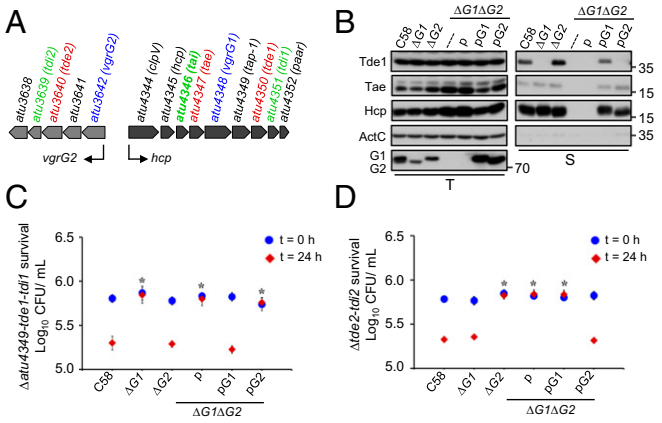

Fig. 1. Genetic organization of *vgrG1* and *vgrG2* and their requirement in specific Tde toxin delivery. (*A*) Genetic organization of *vgrG2* and *hcp* operons of *A. tumefaciens* strain C58. The genes are indicated by the annotated locus tag or designated name adapted from the literature (6, 37). The *vgrG* genes are in blue and the genes encoding the three toxins and their cognate immunity proteins are in red and green, respectively. (*B*) VgrG1 is required for secretion of Tde1 but not Tae. Western blot analysis of the total (T) and secreted (S) proteins from various *A. tumefaciens* strains expressing the plasmid control (p) or indicated plasmid. Protein names and molecular weight markers are indicated at the left and right, respectively. The soluble ActC protein was used as an internal nonsecreted protein control. (*C* and *D*) VgrG1 and VgrG2 are required for Tde1- and Tde2-dependent interbacterial competition activity, respectively. Various *A. tumefaciens* strains shown on the *x* axis were each mixed with Δ*atu4349-tde1-tdi1* (*C*) or Δ*tde2-tdi2* (*D*) at a 10:1 ratio and infiltrated into *N. benthamiana* leaves. The survival of Δ*atu4349-tde1-tdi1* and Δ*tde2-tdi2* collected at 0 and 24-h postinoculation (h) was quantified as cfu. Data are mean ± SEM (*C*, $n = 4$ biological repeats from two independent experiments; *D*, $n = 5$ biological repeats from three independent experiments). Significant difference compared with WT C58 at 24-h postinfiltration (*$P \leq 0.01$). *vgrG1* and *vgrG2* are abbreviated as *G1* and *G2*, respectively.

(Fig. 1*B*). The abolished Tde1 secretion was restored at levels similar to the WT C58 level on *trans*-complementation of *vgrG1* but not *vgrG2* in the Δ*vgrG1*Δ*vgrG2* strain. Therefore, VgrG1 but not VgrG2 is specifically required for the secretion of Tde1 toxin, but VgrG1 or VgrG2 alone is sufficient for Hcp and Tae secretion.

Next, we used an *in planta* interbacterial competition assay to investigate whether the specificity observed for Tde1 toxin secretion reflects its previously observed antibacterial activity (6). Thus, to determine Tde1-dependent antibacterial activity, we mixed the *A. tumefaciens* Δ*atu4349-tde1-tdi1* strain, which is susceptible to killing on injection of Tde1 toxin because of lack of the cognate immunity protein Tdi1 (6), with each of *A. tumefaciens* WT C58, various *vgrG* mutants, and complemented strains. The mixtures were infiltrated into *Nicotiana benthamiana* leaves, and the initial inoculum ($t = 0$ h) and survival (24-h postinfiltration, $t = 24$ h) of Δ*atu4349-tde1-tdi1* harboring the pTrc200 plasmid conferring resistance to spectinomycin was determined by counting cfu on selective media. Survival of Δ*atu4349-tde1-tdi1* was reduced on coinfection with WT C58 or Δ*vgrG2* compared with Δ*vgrG1*Δ*vgrG2* (Fig. 1*C*), which is defective in Hcp and effector secretion (Fig. 1*B*). In contrast, survival of Δ*atu4349-tde1-tdi1* on coinfection with Δ*vgrG1* was similar to that with Δ*vgrG1*Δ*vgrG2* (Fig. 1*C*). Importantly, complementation of *vgrG1* in Δ*vgrG1*Δ*vgrG2* was sufficient for survival of Δ*atu4349-tde1-tdi1* to be reduced similar to WT C58 and Δ*vgrG2* levels (Fig. 1*C*). The combined data indicated that VgrG1 but not VgrG2 is specifically required for Tde1 toxin secretion and Tde1-dependent interbacterial competition activity *in planta*.

VgrG2 Is Specifically Required for Tde2-Dependent Interbacterial Competition Activity *in Planta*. We next tested the role of VgrG2 in Tde2 toxin delivery. Unlike the endogenous expression and secretion

of Tde1 toxin, that of Tde2 toxin was not detectable by Western blot analysis in *A. tumefaciens* (6). Therefore, we used an *in planta* competition assay to test the requirement for VgrG2 in Tde2 toxin delivery. Similar to the design used for Tde1, we coinfected the Δ*tde2-tdi2* deletion strain with each of the *A. tumefaciens* WT C58, various *vgrG* mutants, and complemented strains to determine Tde2-dependent antibacterial activity. The survival of Δ*tde2-tdi2* was markedly reduced on coinfection with WT C58 or Δ*vgrG1* compared with Δ*vgrG1*Δ*vgrG2* or Δ*vgrG2*, and the specific requirement of VgrG2 for Tde2-dependent interbacterial competition activity was further confirmed by *trans*-complementation (Fig. 1*D*). In conclusion, VgrG1 or VgrG2 alone is sufficient for Hcp and Tae secretion, but each VgrG is specifically required for delivery of its cognate Tde toxin for interbacterial competition activity.

C-Terminal Variable/Extension Region of VgrG Is Responsible for Tde Toxin Delivery. Because VgrG1 and VgrG2 are highly conserved at the N-terminal region (1–668 aa) but more divergent at the C-terminal end (669–816 aa in VgrG1 and 669–754 aa in VgrG2) (Fig. S1), we hypothesized that the molecular determinants conferring Tde toxin secretion or delivery specificity are located at the C-terminal variable region of VgrG proteins. To test this hypothesis, we first generated a series of truncated VgrG proteins with C-terminal deletion. We defined VgrG proteins into three regions: highly conserved region A (1–668 aa with only 4-aa differences), variable region B (669–754 aa), and region C representing a C-terminal extension unique to VgrG1 (755–816 aa) (Fig. 2*A*). Thus, two VgrG1 variants, one with deletion of region C (abbreviated as $G1^{AB}$) and one with deletion of both regions B and C ($G1^{A}$), and a VgrG2 variant with deletion of region B ($G2^{A}$), were generated and expressed in the Δ*vgrG1*Δ*vgrG2* strain for type VI secretion and Tde-dependent interbacterial competition assays. As a positive control, expression of full-length VgrG1 in Δ*vgrG1*Δ*vgrG2* enabled the secretion of Hcp, Tae, and Tde1; in contrast, Hcp and effector secretion was not detectable in the VgrG1 variants with deletion of VgrG1 regions B and C ($G1^{A}$) or C ($G1^{AB}$). Similarly, deletion of VgrG2 region B ($G2^{A}$) caused the complete loss of Hcp and Tae secretion, which was detected when full-length VgrG2 was expressed in Δ*vgrG1*Δ*vgrG2* (Fig. 2*B*). Taken together, these results suggested that the C-terminal extension (region C) of VgrG1 and C-terminal variable region (region B) of VgrG2 are required for assembly of a secretion-competent T6SS. The expression of these truncated VgrG variants in Δ*vgrG1*Δ*vgrG2* also caused loss of Tde-dependent interbacterial competition activity *in planta* (Fig. S3 *A* and *B*), which is consistent with their deficiency in mediating type VI secretion activity (Fig. 2*B*).

The complete loss of Hcp secretion in all truncated VgrG variants impeded the identification of molecular determinants in each cognate VgrG specific for Tde toxin delivery. Because protein truncation may cause incorrect protein folding of existing domains and thus lead to a dysfunctional protein, we next used a domain-swapping approach to generate chimeric VgrG proteins and minimize the global structural change of VgrG proteins. A secretion assay revealed that the chimeras $G2^{A}G1^{BC}$, $G2^{AB}G1^{C}$, and $G1^{A}G2^{B}$ but not $G2^{A}G1^{B}$ remained functional in mediating Hcp and Tae secretion (Fig. 2*C*). Among the Hcp and Tae secretion-competent strains, only those expressing $G2^{A}G1^{BC}$ and $G2^{AB}G1^{C}$ but not $G1^{A}G2^{B}$ could mediate Tde1 secretion (Fig. 2*C*), which is consistent with their requirement in mediating Tde1-dependent interbacterial competition activity (Fig. S3*C*). Conversely, only $G1^{A}G2^{B}$ supported Tde2-dependent antibacterial activity at levels similar to full-length VgrG2 (Fig. S3*D*). These results confirmed that Tde1 secretion and delivery specificity require the presence of a C-terminal extension (region C) unique to VgrG1, and the specificity for Tde2 toxin delivery is conferred by the VgrG2 variable region (region B).

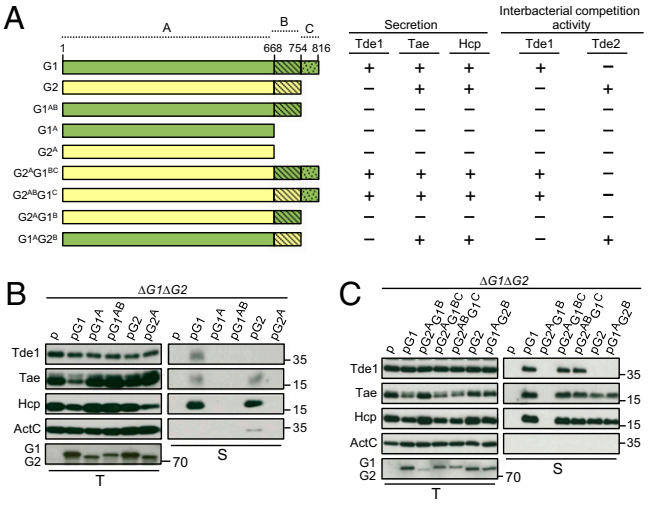

Fig. 2. C-terminal variable/extension region of VgrG is responsible for Tde toxin secretion and interbacterial competition activity. (*A*) Schematic representation of full-length and truncated VgrG1 (green) and VgrG2 (yellow). Highly conserved region (1–668 aa), variable region (669–754 aa), and VgrG1 C-terminal extension (755–816 aa) are denoted as regions A, B, and C, respectively. The name of each variant is indicated at the left. The presence (+) or absence (–) of Tde1, Hcp, and Tae secretion is based on *B* and *C*. Presence (+) and absence (–) of Tde1- and Tde2-dependent antibacterial activity is based on Fig. S3. (*B*) Effect of VgrG variable and C-terminal extension deletion and (*C*) chimeric VgrG variants on type VI secretion. Western blot analysis of total (T) and secreted (S) protein from *A. tumefaciens* Δ*vgrG1*Δ*vgrG2* expressing the plasmid control (p) or indicated plasmid. Protein names and molecular weight markers are indicated at the left and right, respectively. The soluble ActC protein was used as an internal nonsecreted protein control. *vgrG1* and *vgrG2* are abbreviated as *G1* and *G2*, respectively.

Domain Dissection of VgrG in Type VI Secretion and Tde Toxin Delivery. The data from the deletion and chimeras of VgrG variants suggested that the unique C-terminal extension of VgrG1 (region C) and variable region (region B) of VgrG2 are each required for specific Tde toxin delivery. However, the defined regions remain required for assembly of a secretion-competent T6SS because Hcp and Tae secretion are abolished in all VgrG variants with loss of Tde-dependent interbacterial competition activity. Thus, further dissection of the region was needed to identify the molecular determinants dispensable for type VI assembly but specifically required for Tde toxin delivery. Secondary structure prediction by Phyre2 revealed the presence of β-strands connected by loops in the regions; the C-terminal extension of VgrG1 contained seven β-strands connected by seven loops (Fig. 3*A*), whereas the VgrG2 variable region contained eight β-strands connected by eight loops (Fig. 4*A*). Thus, we generated both VgrG1 and VgrG2 C-terminal–truncated variants by stepwise deletion of each putative β-strand and loop from the C-terminal end and expressed these truncated VgrG variants in Δ*vgrG1*Δ*vgrG2*. Deletion analysis was performed until we identified a variant that retained the ability to secrete Hcp or Tae but lost Tde toxin secretion or interbacterial competition activity. Tde1 secretion was no longer detectable with expression of a truncated VgrG1 variant and deletion of the last β-strand β7 ($VgrG1^{812}$), which, however, remained functional to mediate Hcp and Tae secretion (Fig. 3 *A* and *B*). Further analysis of six additional VgrG1 deletion variants revealed that the C-terminal region up to β4 domain is required for Hcp and Tae secretion (Fig. 3 *A* and *B*) (see, for example, $VgrG1^{781}$ and $VgrG1^{785}$). The loss of Tde1 secretion in these VgrG1 deletion variants was also associated with loss of Tde1-dependent interbacterial competition activity as determined by *in planta* competition assay with the three representative deletion variants ($VgrG1^{781}$, $VgrG1^{785}$, and $VgrG1^{812}$) (Fig. 3*C*).

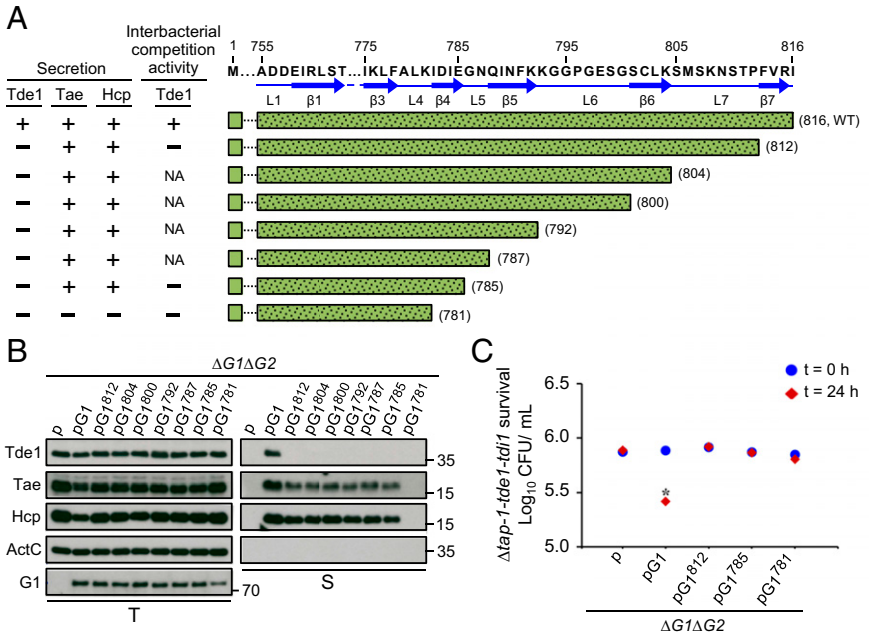

Fig. 3. Effect of VgrG1 C-terminal truncation on type VI secretion and Tde1-dependent interbacterial competition activity. (*A*) Amino acid sequence of VgrG1 C-terminal extension shown with the indicated residue number and predicted β-strands and loops marked with blue solid arrows and lines, respectively. VgrG1 C-terminal truncated variants are shown with green bars filled with dots, and the number in parentheses represents the terminal amino acid of each variant. Presence (+) or absence (–) of Tde1, Hcp, and Tae secretion and Tde1-dependent antibacterial activity is based on Fig. 4 *B* and *C*. NA: not analyzed. (*B*) Western blot analysis of total (T) and secreted (S) proteins from *A. tumefaciens* Δ*vgrG1*Δ*vgrG2* expressing the plasmid control (p) or indicated plasmid. Protein names and molecular weight markers are at the left and right, respectively. The soluble ActC protein was used as an internal nonsecreted protein control. (*C*) Effect of VgrG1 C-terminal truncation on Tde1-dependent interbacterial competition activity. Various *A. tumefaciens* strains shown on the *x* axis were mixed with Δ*tap-1-tde1-tdi1* at a 10:1 ratio and infiltrated into *N. benthamiana* leaves. The survival of Δ*tap-1-tde1-tdi1* collected at 0 and 24 h was quantified as cfu. Data are mean ± SEM ($n = 5$ biological repeats from two independent experiments). Significant difference compared with Δ*vgrG1*Δ*vgrG2* (Δ*G1*Δ*G2*) at 24-h postinfiltration (*$P \leq 0.01$). *vgrG1* and *vgrG2* are abbreviated as *G1* and *G2*, respectively.

Thus, we identified that the VgrG1 C-terminal 31-aa region (786–816 aa; C31), the region downstream of β4, is required for Tde1 toxin secretion and delivery specificity but is not essential for assembly of a secretion-competent T6SS.

For VgrG2, the expression of a VgrG2 variant with deletion of the last β-strand β8 ($VgrG2^{742}$) in Δ*vgrG1*Δ*vgrG2* already caused complete loss of Hcp and effector secretion (Fig. 4*B*). Thus, we generated three additional VgrG2 variants with 1-aa, 5-aa, and 8-aa C-terminal truncation ($VgrG2^{753}$, $VgrG2^{749}$, $VgrG2^{746}$). Strikingly, Hcp secretion was largely reduced and Tae secretion was barely detected with expression of each of the three VgrG2 variants compared with the WT VgrG2 (Fig. 4*B*). Not surprisingly, Tde2-dependent interbacterial competition activity was not detectable in all four strains expressing these VgrG2 variants (Fig. 4*C*). These data suggest that the last C-terminal 8 aa (747–754 aa; C8) in VgrG2 is important but not essential for the assembly of a secretion-competent T6SS and is required for Tde2 toxin delivery to confer Tde2-dependent interbacterial competition activity.

Widespread Genetic Linkage of Cognate *vgrG* with Distinct Adaptor/Chaperone and Effector Genes in Proteobacteria. Both Tde1 and Tde2 belong to a toxin_43 superfamily defined by Pfam: Tde1 belongs to class 1, containing only an identifiable toxin_43 domain, and Tde2 belongs to class 3, harboring the N-terminal DUF4150 followed by a toxin_43 domain located in the C terminus (6). Because the *tde-tdi* toxin-immunity gene pair is well conserved in Proteobacteria and is often genetically linked with *vgrG* (6), we wondered about a specific genetic linkage for *vgrG1* with *tde1-tdi1* and *vgrG2* with *tde2-tdi2* in Proteobacteria other than *A. tumefaciens*. Through database searches, we identified 18 putative orthologs of *tde1* (defined as ≤300-aa long and containing solely a toxin_43 domain) and 5 putative *tde2* orthologs (defined by their N-terminal DUF4150 and C-terminal toxin_43 domains) (Fig. S4). Because DUF4150 exhibits similarity to the PAAR domain, which caps the end of the β-helix of a VgrG spike and may function as a piercing tip to facilitate secretion of a broad range of toxins (28), we extended our search and identified seven Tde2-like (Tde2L) proteins defined by their N-terminal PAAR and C-terminal toxin_43 domains. Furthermore, a genetic context survey revealed that all identified *tde* homologs were genetically linked to immunity genes (i.e., *tdi*). Among the 18 *tde1-tdi1* gene pairs, 5 were genetically associated with *vgrG* and confined to bacteria belonging to α-Proteobacteria, in which these VgrG proteins all contain a C-terminal sequence highly conserved with the C31 region (786–816 aa) of *A. tumefaciens* C58 VgrG1 (Fig. 5 and Fig. S5). Strikingly, all five *tde2-tdi2* and seven *tde2l-tdi2l* gene pairs were genetically linked to *vgrG* and present in bacteria across α-, β-, and γ-Proteobacteria, in which these VgrG proteins are shorter and possess the conserved C8 sequence (747–754 aa) of *A. tumefaciens* C58 VgrG2 (Fig. 5 and Fig. S5). Based on the domain organization and similarity, the *tde1*-linked *vgrG* genes are defined as *vgrG1* orthologs and *tde2*/*tde2l*-linked *vgrG* genes are *vgrG2* orthologs.

Intriguingly, in addition to the tight genetic linkage among *vgrG-tde-tdi* homologs, our gene context analysis also identified additional genes conserved in these gene clusters. For *vgrG1*-type gene clusters, a gene encoding for a protein with the DUF4123 domain known as an adaptor/chaperone (6, 32, 33) is always found between *vgrG1* and *tde1* (Fig. 5*A*). Furthermore, except for the gene cluster found in *Inquilinus limosus*, all *vgrG1*-type gene clusters have a PAAR-domain–containing gene downstream of *tdi1*. For *vgrG2*-type gene clusters, a gene encoding for a DUF2169-domain–containing protein is always found between *vgrG2* and *tde2* (Fig. 5*A*). The conservation in gene cluster organization across diverse Proteobacterial lineages suggests that individual genes within the same

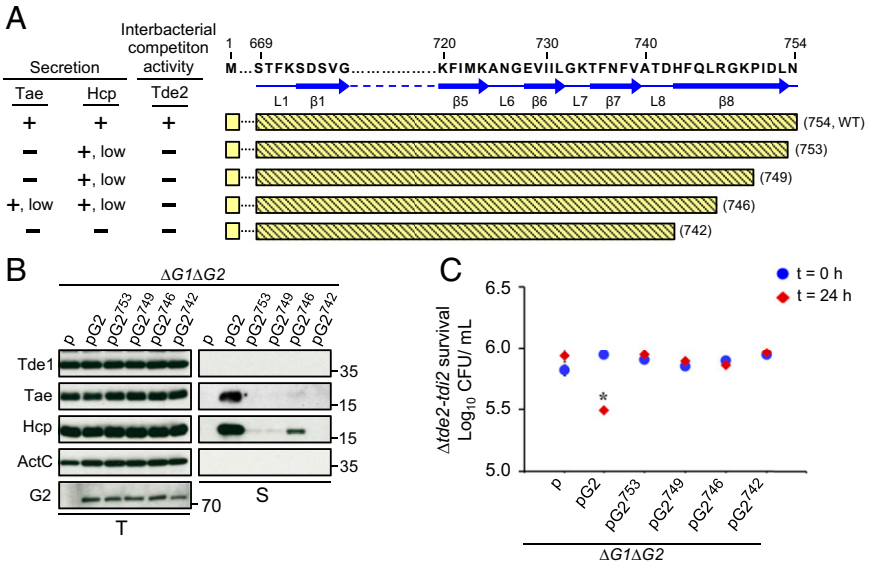

Fig. 4. Effect of VgrG2 C-terminal truncation on type VI secretion and Tde2-dependent interbacterial competition activity. (*A*) Amino acid sequence of VgrG2 C-terminal variable region is shown with the indicated residue number, and the predicted β-strands and loops are marked with blue solid arrows and lines, respectively. VgrG2 C-terminal truncated variants are shown with yellow bars, and the numbers in parentheses represent the terminal amino acid of each variant. Presence (+) or absence (–) of Hcp and Tae secretion and Tde2-dependent antibacterial activity is based on Fig. 3 *B* and *C*. (*B*) Western blot analysis of total (T) and secreted (S) protein from *A. tumefaciens* Δ*vgrG1*Δ*vgrG2* expressing the plasmid control (p) or indicated plasmid. Protein names and molecular weight markers are indicated at the left and right, respectively. The soluble ActC protein was an internal nonsecreted protein control. (*C*) Effect of VgrG2 C-terminal truncation on Tde2-dependent interbacterial competition activity. Various *A. tumefaciens* strains shown on the *x* axis were mixed with Δ*tde2-tdi2* at a 10:1 ratio and infiltrated into *N. benthamiana* leaves. The survival of Δ*tde2-tdi2* collected at 0 and 24 h was quantified as cfu. Data are mean ± SEM ($n = 5$ biological repeats from two independent experiments). Significant difference compared with Δ*vgrG1*Δ*vgrG2* (Δ*G1*Δ*G2*) at 24-h postinfiltration (*$P \leq 0.01$). *vgrG1* and *vgrG2* are abbreviated as *G1* and *G2*, respectively.

cluster may be functionally linked, which prompted our further investigation on the roles of these adapter/chaperone-like proteins in determining VgrG-Tde specificity.

Tap-1 (Atu4349) and PAAR Protein Atu4352 Are Required for Tde1-Dependent Antibacterial Activity and Tde1 Secretion. Because of the conservation of *vgrG1-atu4349-tde1-tdi1-atu4352* genetic linkage in α-Proteobacteria (Fig. 5*A*), we hypothesized that in addition to VgrG1, Atu4349 and Atu4352 may play roles in Tde1 translocation. This hypothesis was indeed supported by our previous observation that the DUF4123-domain–containing protein Atu4349 interacts directly with Tde1 to form a complex in *E. coli* and stabilizes Tde1 in *A. tumefaciens* C58 (6), and two recent studies identifying a *V. cholerae* DUF4123-domain–containing protein, Tap-1/Tec, required for loading a specific effector onto cognate VgrG for secretion (32, 33). Thus, we first determined the role of *atu4349* (named *tap-1*) and *atu4352* (named *paar*) in Tde1 secretion and Tde1-dependent antibacterial activity. Because Tde1 and Tde2 but not Tae toxins are responsible for detectable antibacterial activity (6), we used *E. coli* DH10B-expressing *tdi2* as a target strain to determine Tde1-dependent antibacterial activity. As controls, WT C58 and Δ*tde2-tdi2* but not Δ*tap-1-tde1-tdi1* killed the Tde1 toxin-sensitive *E. coli* target cell efficiently, so the observed *E. coli* killing activity was contributed by Tde1 toxin (Fig. 6*A*). Deletion of *tap-1* abolished the antibacterial activity, and the *trans* expression of *tap-1* on pTrc200 partially restored the Tde1-dependent antibacterial activity; this partially restored phenotype may be a result of the lower protein levels of Tap-1 synthesized by *trans* expression or the *cis* expression of *tap-1* with *tde1* being critical for efficient Tde1 toxin delivery. Indeed, the expression of *tap-1-tde1-tdi1* on pTrc200 in Δ*tap-1* was able to fully restore Tde1-dependent antibacterial activity similar to WT C58 and Δ*tde2-tdi2*. Consistent with the role of Tap-1 in stabilizing Tde1 and Tde1-dependent antibacterial activity, the intracellular Tde1 protein level was reduced and its secretion completely abolished in Δ*tap-1*, whereas *trans* expression of *tap-1* or *tap-1-tde1-tdi1* could partially or completely restore Tde1 secretion (Fig. 6*D*).

Next, we determined the role of the *paar* gene in Tde1 toxin delivery. Tde1-dependent antibacterial activity was highly compromised but not completely abolished in Δ*paar* (Fig. 6*B*), which is consistent with reduced Tde1 secretion in the absence of this PAAR protein (Fig. 6*E*). *Trans* expression of *paar* in Δ*paar* fully restored both Tde1 secretion and the Tde1-dependent antibacterial activity phenotype. Of note, Hcp and Tae secretion remained unaffected in Δ*tap-1* but slightly affected in Δ*paar*. Taking these data together, we conclude that both Tap-1 and PAAR play critical roles for Tde1 secretion, facilitating *A. tumefaciens* T6SS to engage in Tde1-dependent antibacterial activity.

Atu3641, a DUF2169-Containing Protein, Is Required for Tde2-Dependent Antibacterial Activity. In addition to the conserved genetic linkage of *vgrG1-tap-1-tde1-tdi1-paar* orthologs found in α-Proteobacteria (Fig. 5*A*), *atu3641*, encoding a DUF2169-domain–containing protein, is 100% conserved with genetic linkage to *vgrG2* and *tde2/tde2l* orthologs across many Proteobacterial classes we identified. Thus, we performed Tde2-dependent antibacterial activity assay with DH10B expressing *tdi1* used as a target strain (Fig. 6*C*). As controls, WT C58 and Δ*tap-1-tde1-tdi1* killed the Tde2 toxin-sensitive *E. coli* target cell efficiently, but Δ*tde2-tdi2* could not, so the observed antibacterial activity was contributed by Tde2 toxin. The deletion of *atu3641* abolished the antibacterial activity and the *trans* expression of Atu3641 tagged with hemagglutinin (HA) in Δ*atu3641* fully restored the Tde2-dependent antibacterial activity. Because the secretion of Tde1, Tae, and Hcp was not affected in Δ*atu3641* and Atu3641-HA was not detectable in secretion fraction (Fig. 6*F*), we suggest that Atu3641 plays no roles in the global secretion function of T6SS but is specifically required for Tde2 translocation to exert antibacterial activity.

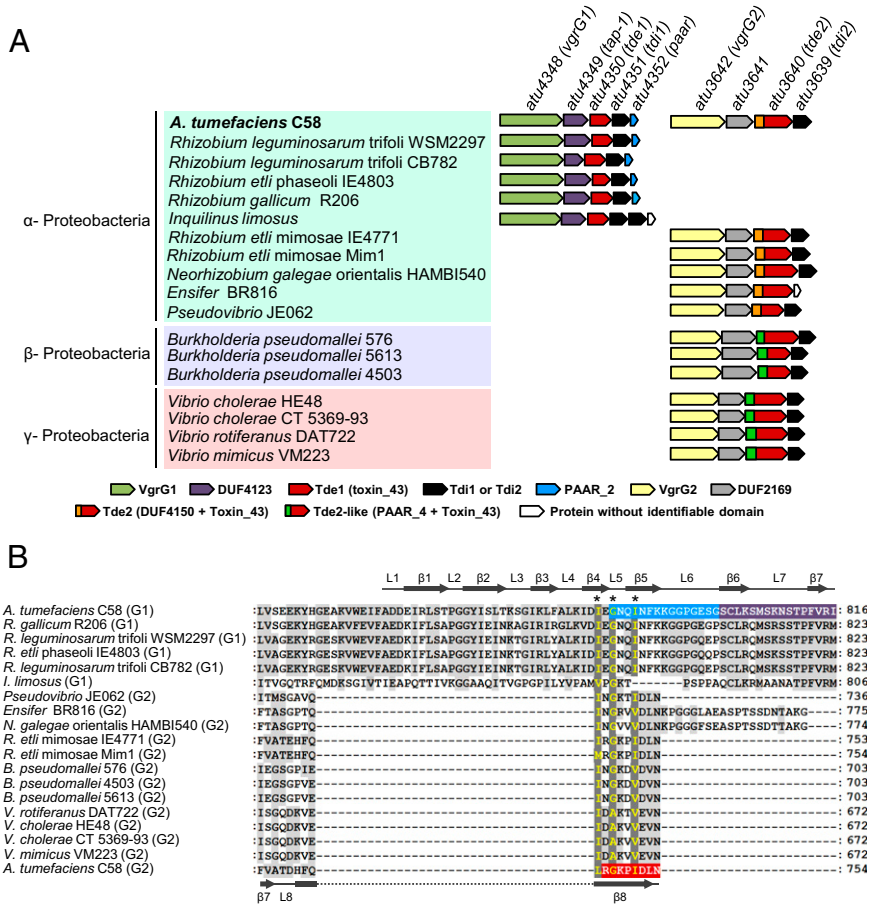

Fig. 5. (*A*) Conservation of the *vgrG1-tap-1-tde1-tdi1-paar* and *vgrG2-atu3641-tde2-tdi2* gene clusters in Proteobacteria. Bacteria belonging to different proteobacterial classes are shaded with different colors. Genetic organization at right of each bacterium was deduced from manual inspection of respective bacterial genome and color-coded by the presence of a conserved protein domain as predicted by an NCBI-CD search algorithm (39). The locus tags/names of *A. tumefaciens* C58 genes are indicated and the color-coded protein domains are listed and drawn to scale. (*B*) C-terminal amino acid sequence alignment of *tde*-associated *vgrG* homologs. C-terminal regions of identified VgrG1 and VgrG2 homologs aligned in Fig. S5 are presented. The amino acid residues in dark gray represent highly conserved residues and in light gray, partially conserved residues. Numbers at the right represent the terminal amino acid residue of each aligned VgrG homolog. The VgrG1 C31 sequence is shaded in blue (region required for PAAR binding) and purple (region dispensable for PAAR but required for interacting with Tap-1–Tde1 complex) and the VgrG2 C8 sequence is shaded in red. A common I/LxG/AxxI/V motif located at the boundary uncoupling Hcp and Tde toxin delivery is highlighted and indicated by asterisks (*). The predicted secondary structure of *A. tumefaciens* C58 VgrG1 and VgrG2 is indicated at the top and bottom, respectively.

Protein–Protein Interaction Studies of VgrG1, Tap-1, Tde1, and PAAR. With our previous evidence that Tap-1 interacts with and stabilizes Tde1 (6), which requires VgrG1, Tap-1, and PAAR for translocation (Fig. 6), we hypothesized that these proteins facilitate Tde1 toxin delivery by interacting with one another. To test this hypothesis, we used coimmunoprecipitation (co-IP) in *A. tumefaciens* to determine whether these proteins interact in vivo (Fig. 7). The cleared cell lysates prepared from dimethyl 3,3′-dithiobispropionimidate (DTBP) –cross-linked *A. tumefaciens* cells served as an input fraction, which was incubated with antibody specific to the VgrG1 C-terminal extension (named VgrG1^{C}), Tde1, or HA (for PAAR protein tagged with HA epitope) for co-IP. The antibody against RpoA (RNA polymerase α-subunit) was used as a negative control. Tde1 and Tap-1 coprecipitated with VgrG1 by anti-VgrG1^{C} antibody, whereas VgrG1 and Tap-1 coprecipitated with Tde1 by anti-Tde1 antibody in WT C58, which suggests physical interactions among VgrG1, Tap-1, and Tde1. Because a negative control protein, RpoA, did not coprecipitate with anti-VgrG1^{C} or anti-Tde1 and none of these proteins was coprecipitated by anti-RpoA, the observed interactions among VgrG1, Tap-1, and Tde1 were specific (Fig. 7*A*). To determine the interaction relationship among these three proteins, we performed further co-IP experiments that lack one protein at a time. Tap-1 retained its interaction with Tde1 in the absence of VgrG1 or PAAR, which is consistent with the Tap-1–Tde1 complex formation in *E. coli* (6). In contrast, VgrG1 no longer interacted with Tde1 in Δ*tap-1* and lost interaction with Tap-1 in the absence of Tde1. These results suggest that the Tap-1–Tde1 complex formation is required for their interaction with VgrG1 to form this ternary complex. However, the VgrG1–Tap-1–Tde1 complex formation did not require PAAR because they coprecipitated with each other in Δ*paar.* Cocrystallography study showed that PAAR protein interacts directly with the last β-strand of a gp5-VgrG chimera to sharpen the VgrG tip (28), so we tested whether PAAR interacts with the VgrG1–Tap-1–Tde1 complex. When PAAR-HA was used for co-IP by anti-HA antibody, VgrG1, Tap-1, and Tde1 were coprecipitated with PAAR-HA on incubation of the input fraction prepared from Δ*paar* (pPAAR-HA) (Fig. 7*B*). None of these proteins was detected from the elute fraction of the negative control, the Δ*paar* strain expressing plasmid (p) alone, which suggests specific interactions of PAAR-HA with VgrG1, Tap-1, and Tde1. We also observed that PAAR-HA retained its interaction with VgrG1 in the absence of Tap-1 or Tde1, so VgrG-PAAR-HA forms a complex independent of Tap-1 and Tde1. However, Tap-1 and Tde1 were no longer coprecipitated with PAAR-HA in Δ*vgrG1*, Δ*tap-1*, and Δ*tde1*. Therefore, Tap-1 and Tde1 require each other

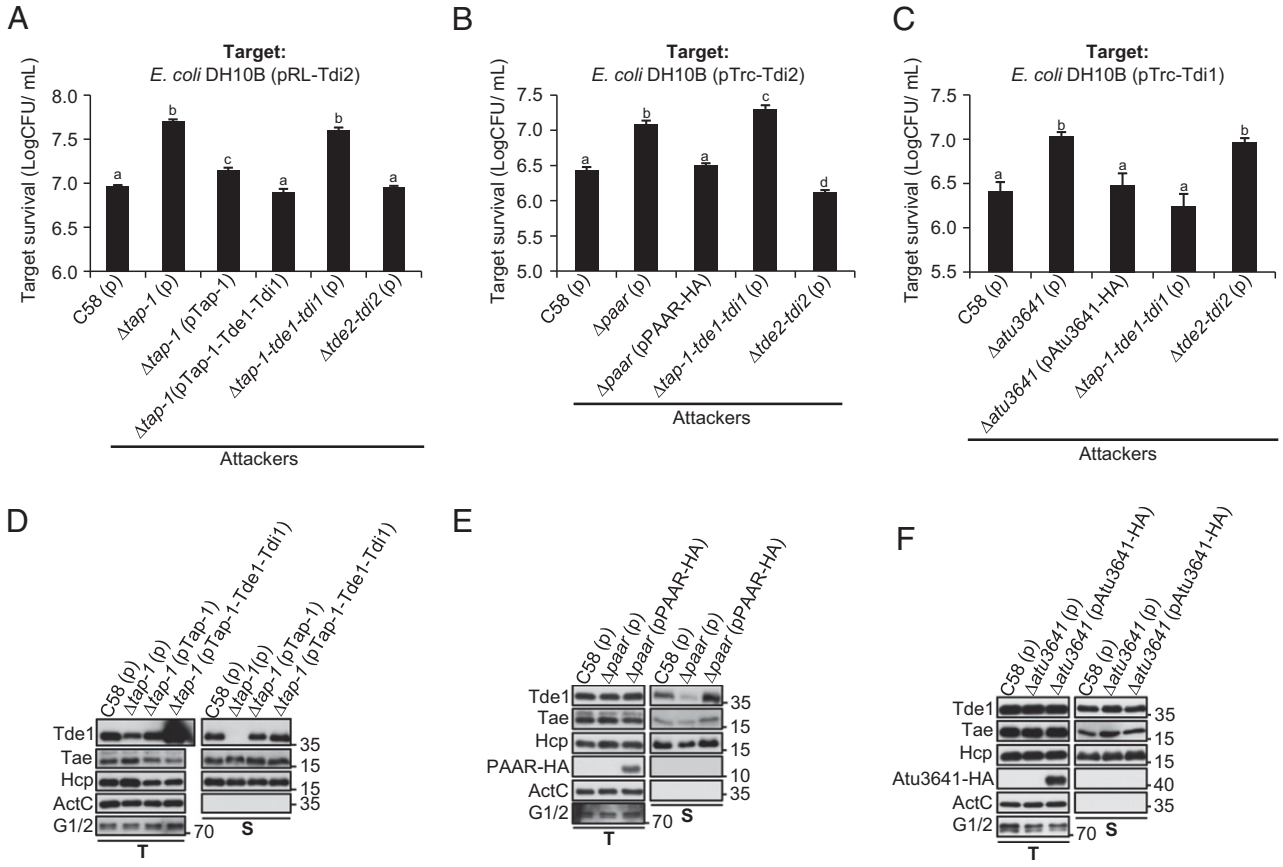

Fig. 6. The effect of *tde*-associated genes *tap-1*, *paar*, and *atu3641* for cognate Tde effector translocation. Requirement of *tap-1* (*A* and *D*) and *paar* genes (*B* and *E*) in Tde1-dependent antibacterial activity and Tde1 secretion; requirement of *atu3641* in Tde2-dependent antibacterial activity (*C*) and type VI secretion (*F*). (*A–C*) *E. coli* killing assay in which attacker *A. tumefaciens* strains containing the plasmid only (p) or expressing the indicated genes shown on the *x* axis were mixed with *E. coli* DH10B cells expressing *tdi1* or *tdi2* at a 30:1 ratio for competition. The survival of *E. coli* cells was quantified as cfu and shown on the *y* axis. Data are mean ± SEM ($n = 5$ biological repeats from two independent experiments) computed by one-way ANOVA. Different letters above the bar indicate significant difference ($P < 0.05$) determined by Tukey's HSD test. (*D–F*) Western blot analysis of the total (T) and secreted (S) proteins from various *A. tumefaciens* strains expressing the plasmid control (p) or indicated gene. Protein names and molecular weight markers are indicated at the left and right, respectively. The soluble ActC protein was used as an internal nonsecreted protein control.

and VgrG1 to interact with PAAR, whereas the VgrG1-PAAR interaction does not require Tap-1 or Tde1 (Fig. 7*E*). Taken together, these data strongly suggest the formation of a Tap-1–Tde1–VgrG1–PAAR complex in which the Tap-1–Tde1 complex forms before interaction with VgrG1, which also associates with PAAR.

Distinct Regions in VgrG1 C31 Required for the Tap-1–Tde1 Complex and PAAR Binding. Because the C31 peptide of VgrG1 is not essential for Hcp and Tae secretion but is specifically required for Tde1 secretion and Tde1-dependent antibacterial activity specificity, we first tested whether this C31 region is required for the interaction of VgrG1 with Tap-1, Tde1, and PAAR. Full-length VgrG (pG1) or C31-truncated VgrG1 ($G1^{785}$) was expressed in Δ*vgrG1*Δ*vgrG2* for co-IP experiments with specific antibody for VgrG1, Tde1, or RpoA (a negative control). As expected, full-length VgrG1, Tap-1, and Tde1 were coprecipitated by anti-$VgrG1^{C}$ or anti-Tde1 antibody, whereas RpoA was not (Fig. 7*C*). As controls, neither Tde1 nor Tap-1 was coprecipitated by anti-RpoA, but a weak but detectable VgrG1 signal was coprecipitated by anti-RpoA antibody, likely because of higher levels of VgrG1 expressed from pG1 than endogenous levels in WT C58. On co-IP experiments for $VgrG1^{785}$, only Tap-1 but not $VgrG1^{785}$ was specifically coprecipitated with Tde1 by anti-Tde1 antibody, so the C31 region is required for VgrG1 to interact with the Tap-1–Tde1 complex. Furthermore, this C31 region is also required for VgrG1 to interact with PAAR because full-length VgrG1 but not $VgrG1^{785}$ could be coprecipitated with PAAR-HA by anti-HA antibody (Fig. 7*D*). Interaction of Tap-1 and Tde1 with PAAR-HA was also lost when VgrG1 is lacking this C31 region. Thus, C31 is required for VgrG1 to interact with the Tap-1–Tde1 complex and PAAR. Analysis of additional truncated VgrG1 variants further revealed that PAAR-HA coprecipitated efficiently with the $VgrG1^{800}$, $VgrG1^{804}$, and $VgrG1^{812}$ variants but not the $VgrG1^{792}$ variant. In contrast, no coprecipitation of Tde1 and Tap-1 could be detected in all truncated VgrG variants except WT VgrG1 (Fig. 7*D*). Thus, whereas the entire C31 segment of VgrG1 is required for binding with Tap-1-Tde1 complex, only the first 15 aa (L5, β5, and L6) of this region is required for PAAR binding.

Discussion

T6SS deploys the components of its phage tail-like structure, tube component Hcp and spike protein VgrG, for delivery of diverse effectors. Here, we identified the T6SS components specifically required for effector transport and the molecular determinants of the cognate VgrG proteins in Tde toxin delivery in *A. tumefaciens* strain C58. This conserved type VI effector delivery mechanism is governed by a divergent C-terminal end of VgrG protein, in which the C31 region of VgrG1 is required for interacting with an adaptor/chaperone–effector complex (Tap-1–Tde1) and PAAR

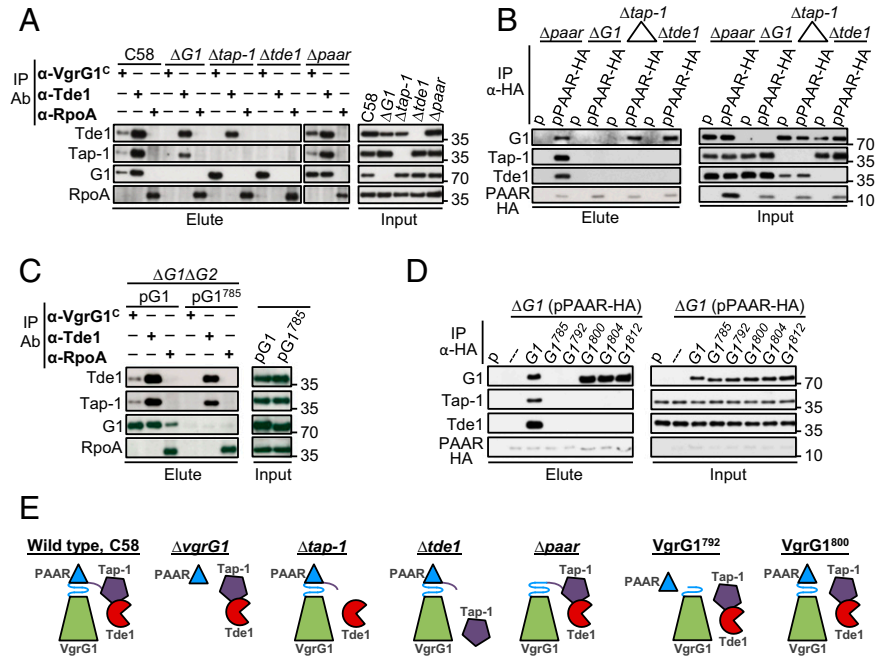

Fig. 7. Interactions of VgrG1, Tap-1, Tde1, and PAAR proteins. Co-IP of WT *A. tumefaciens* C58 and indicated mutant strains (*A*) or Δ*vgrG1*Δ*vgrG2* (Δ*G1*Δ*G2*) expressing full-length *vgrG1* (*G1*) and with the *vgrG1* C31 deletion variant (*G1*^{785}) (*C*) by using α-VgrG1 C-terminal epitope and α-Tde1 antibodies. α-RpoA antibody was used as a negative control. Co-IP of various mutants by using strains expressing pRL662 plasmid (p) only or PAAR-HA (*B*) or Δ*G1*(pPAAR-HA) expressing full-length VgrG1 (G1) or each of truncated VgrG1 variants (*D*) by anti-HA antibody. The resulting total protein extract was used as input for Co-IP. Coprecipitated proteins were detected by Western blot analysis with antiserum specific to indicated proteins. Proteins in input and elute fractions were detected by Western blot analysis. Protein names and molecular weight markers are indicated at the left and right, respectively. (*E*) A summary model of protein–protein interactions. Each protein is color-coded and C31 of VgrG1 is presented as β-helix consisting L5-β7 (L5-β5-L6 in blue and β6-L7-β7 in purple) at tip of VgrG spike.

protein for Tde1 translocation across bacterial membranes to extracellular milieu and delivery into target cells. This critical role of the VgrG divergent C terminus in specific effector delivery is also experimentally supported by two recent reports. Unterweger et al. showed that a 37-amino acid-long linker sequence connecting gp27–gp5 and actin cross-linking domains of *V. cholerae* VgrG1 is required for TseL antibacterial activity without affecting Hcp secretion (33). However, whether this linker sequence is required for Tap-1 binding to load effector on VgrG1 spike has remained unknown. Interestingly, Flaugnatti et al. recently reported the direct binding of Tle1 phospholipase effector with C terminus of VgrG in *E. coli* Sci-1 T6SS without bridging by an adaptor protein (11). Taken together, these recent reports and our new findings indicate that the divergence in C-terminus sequences have allowed distinct mechanisms for effector loading and delivery among VgrG proteins.

The combined data from deletion and domain-swapping analysis indicate that the C-terminal extension (region C) of VgrG1 and the variable region (region B) of VgrG2 confer specificity for Tde toxin delivery (Fig. 2). In contrast, the highly conserved N-terminal region (1–668 aa) does not contribute to the specificity of effector transport because swapping this region between VgrG1 and VgrG2 did not change the specificity. Because this variable region (region B) is part of the gp5 domain, as expected, removal of region B in both VgrG1 and VgrG2 abolished Hcp and Tae secretion. The C-terminal extension (region C) is unique to VgrG1, but part of this region C (755–785 aa) is still required for mediating Hcp and Tae secretion (Fig. 3). Because deletion of C31 region (containing L5–7 and the last three β-strands β5–7) in VgrG1 still maintained the ability to mediate near WT-level of Hcp and Tae secretion but caused the complete loss of Tde1 secretion and Tde1-depdendent interbacterial competition activity, the VgrG1 C31 sequence plays a specific role governing Tde1 toxin delivery. In contrast, the C-terminal 8-aa sequence (C8, including part of the last β-strand β8) of VgrG2 is critical but not essential in Hcp and Tae secretion. Because the deletion of the C8 sequence in VgrG2 led to very low Hcp and Tae secretion, the loss of Tde2-dependent interbacterial activity is contributed by both inefficient assembly of secretion-competent T6SS and its specific role in Tde2 translocation. Taken together, VgrG1, by evolving into a longer protein with a C-terminal extension, acquires an extended C31 sequence that is nearly dispensable for T6SS assembly but specifically confers Tde1 toxin delivery. However, the VgrG2 protein with the N-terminal gp27 domain and C-terminal gp5 domain constituting the entire protein, contains the C-terminal C8 sequence with functions in both T6SS assembly and Tde toxin transport specificity.

In addition to VgrG, a few additional T6SS components were shown to participate in effector translocation. One is PAAR protein, which interacts directly with the last β-strand of a gp5–VgrG chimera and can act as an adaptor between VgrG and effector to facilitate secretion of a broad range of T6SS toxins (28). Others include the DUF4123-domain–containing protein Tap-1/Tec for loading a specific effector onto cognate VgrG for delivery in *V. cholerae* (32, 33) and EagR accessory protein specifically required for deployment of its associated Rhs effector in *Serratia marcescens* (8). We found that all *tde1* orthologs are linked to an upstream *tap-1*, and except for in *I. limosus*, are associated with a downstream *paar* gene (Fig. 5*A*). As for Tde2 homologs harboring an N-terminal PAAR-like DUF4150 domain and Tde2L homologs containing an N-terminal PAAR domain, followed by a C-terminal toxin_43 domain, all *tde2*/*tde2l* orthologs are 100% linked to upstream genes encoding a DUF2169 domain. Such strong conservation indeed reflects their critical roles in translocation of their genetically linked Tde effectors, in which both Tap-1 and DUF2169 are not required for global type VI secretion activity but play an essential and specific role in Tde toxin delivery (Fig. 6). According to the Pfam database, DUF2169-domain–containing proteins are present in at least 120 Gram-negative bacteria belonging to different phyla (Fig. S6*A*). Similar to *tap-1* genes that are

genetically linked to *tde1* orthologs (6) and also associated with other known or putative effector genes (32, 33), we also found that some of the DUF2169-encoding genes are located upstream of putative effector genes other than *tde2*/*tde2l* (Fig. S6*B*). Importantly, many of these putative effectors encode an N-terminal PAAR or DUF4150 domain, so we hypothesized that DUF2169 may serve as an adaptor or chaperone in binding with the N-terminal PAAR or PAAR-like domain of its cognate effector to the VgrG tip for translocation. Because the cellular concentration of WT Tde2 was below the detection level on Western blot analysis (6), it is not feasible to determine whether the DUF2169 protein Atu3641 could directly interact with the endogenous WT Tde2 in *A. tumefaciens*. However, we are able to show a role of Atu3641 in stabilizing Tde2, in which intracellular protein levels of the Strep-tagged Tde2 variant with catalytic site mutations ($Tde2^{H439A,\ D442A}$) were enhanced when coexpressed with Atu3641-HA (Fig. S6*C*). Because the aforementioned functions of Atu3641 are similar to Tap-1, we proposed that Atu3641 may function as a chaperone to stabilize Tde2 and perhaps is an adaptor for Tde2 translocation, but further experimental evidence (such as Atu3641–Tde2 interaction) is required to confirm its function as chaperone.

Based on the co-IP experiments in WT C58 and various mutants, we present an interaction model (Fig. 7*E*), suggesting a Tap-1–Tde1–VgrG1–PAAR complex formation, in which both the Tap-1–Tde1 complex and VgrG1–PAAR complex can form in the absence of each other. The evidence of the reciprocal requirement of Tap-1 and Tde1 for interacting with VgrG1 suggests that the Tap-1–Tde1 complex must form before interacting with VgrG1, which is likely present as a preformed complex with PAAR at its tip. However, preloading of PAAR to VgrG1 is not required for VgrG1–Tap-1–Tde1 complex formation. Strikingly, the C31 region of VgrG1 is required for interacting with both the Tap-1–Tde1 complex and PAAR, which supports a direct role of this VgrG1 C31 terminus for loading an adaptor/chaperone-effector complex and piercing tip protein, PAAR.

Multiple alignments of all *tde*-linked *vgrG* genes at the protein level further revealed a conserved I/LxG/AxxI/V motif at the boundary uncoupling Hcp and Tde toxin delivery. Shneider et al. (28) postulated that the VgrG β-strand extends to the very C terminus of the protein or terminates with a Gly/Ser-rich stretch for bending away from the tip to provide the β-strand blunt end for interacting with PAAR and PAAR-like domains in effector delivery. Thus, β5, the β-strand connected to the Gly/Ser-rich stretch (L6) of VgrG1 or, broadly, the β4–L5–β5 region covering this I/LxG/AxxI/V conserved motif, may be the binding site of the PAAR protein encoded downstream of *tde1*. The extended C terminus beyond β5 of VgrG1 may provide the binding site for an adaptor/chaperone–effector complex. The co-IP data demonstrated that the L5, β5, and L6 regions in C31 are required for PAAR binding. In comparison, the C16 region harboring β6, L7, and β7 is dispensable for PAAR binding but is required for interaction with the Tde1–Tap-1 complex. To our knowledge, these results are the first experimental evidence for the distinct binding sites of adaptor/chaperone–effector complex and PAAR and form the foundation of our model (Figs. 5*B* and 7*E*). As for VgrG2, we propose that β8 (exact I/LxG/AxxI/V motif), the last β-strand of VgrG2, may interact with the DUF4150 domain of Tde2 and the PAAR domain of Tde2L. The blockage of Tde2 toxin delivery by fusing the VgrG1 C-terminal extension to full-length VgrG2 (Fig. 2) indeed supports that this β-strand must be exposed for binding with an effector or adaptor protein.

It is also interesting to note that deletion of *paar* reduced but did not completely abolish the secretion of Tde1, as well as Tae and Hcp (Fig. 6). Because the VgrG1–Tap-1–Tde1 complex can form efficiently without PAAR for low but detectable Tde1 secretion and antibacterial activity, PAAR binding to the VgrG may not be required but can facilitate assembly or translocation of the Hcp tube loaded with a VgrG-associated effector complex across membranes. This result agrees with the modest or marked reduction of Hcp secretion in the single or multiple *paar* deletion mutants in *V. cholerae* and *Acinetobacter* (28), in which the authors also suggested the role of PAAR in assembly of the T6SS complex by nucleating the folding of VgrG trimers or regulating VgrG incorporation into T6SS nanomachine. Because of the complexity of multiple VgrG and PAAR proteins involved in type VI effector translocation, future work in identifying each of distinct effector-loaded VgrG complexes will be critical to elucidate the roles and molecular details underlying PAAR and effector loading onto VgrG tip in effector translocation mechanisms.

Experimental Procedures

Bacterial Strains, Growth Conditions, and Molecular Cloning Techniques. The strains/plasmids and primers used in this study are in Tables S1 and S2. Unless indicated, *A. tumefaciens* strains were grown in 523 medium at 28 °C. *E. coli* strains were grown in Luria Bertani (LB) medium at 37 °C, as described previously (6, 37). When required, the following antibiotics were used: gentamycin (50 μg/mL^{-1} for *A. tumefaciens*, 30 μg/mL^{-1} for *E. coli*) and spectinomycin (200 μg/mL^{-1}). DNA preparation, PCR, and cloning procedures were described in detail in *SI Experimental Procedures*.

Interbacterial Competition Assay. An *in planta* bacterial competition assay was performed as described previously (6). Briefly, *A. tumefaciens* strains were transformed with gentamycin resistance-conferring pRL662 plasmid or spectinomycin resistance-conferring pTrc200 plasmid for selecting surviving cells. The so-called attacker and target strains were mixed in one-half Murashige and Skoog (MS) medium (pH 5.7) at a 10:1 ratio and infiltrated into leaves of 6- to 7-wk-old *N. benthamiana* plants by use of a needleless syringe. The infiltrated zone at 0 and 24-h postinfiltration was collected and the competiton outcome of each strain was quantified by counting cfus in triplicate on LB agar plates containing the appropriate antibiotics. Antibacterial activity assay with *E. coli* used as a target was performed as described previously (6). In brief, overnight-grown *A. tumefaciens* and *E. coli* strains harboring appropriate plasmid were adjusted to OD_{600} 0.1 and incubated at 25 °C for 7 h before coincubation. *A. tumefaciens* and *E. coli* cells were mixed at a 1:30 ratio and spotted onto LB agar plates. Where applicable, the mixture was spotted onto a LB agar plate containing 0.5 mM isfopropyl-β-D-thiogalactopyranoside (IPTG) to induce expression from the pTrc200 plasmid. At 16-h postincubation at 25 °C, the spots were harvested, serially diluted and plated on LB agar plate containing an appropriate antibiotic to quantify surviving *E. coli* cfu. Data are expressed as mean ± SEM from at least three biological repeats obtained from two or three independent experiments. Significant growth differences for each strain compared with the indicated control at 24-h postinfiltration was computed by one-way ANOVA and Tukey's honestly significance difference (HSD) test (statistica.mooo.com/).

Type VI Secretion Assay. The type VI effector secretion assay was performed as described previously (6). Total and secreted proteins were fractionated by SDS/PAGE and transferred onto a PVDF membrane by using a transfer apparatus (Bio-Rad). Unless indicated, the membrane was probed with primary antibody against VgrG1, which recognizes both VgrG1 and VgrG2 (1:1,000) (37), Tde1 epitope (1:4,000) (6), Hcp (1:2,500) (34), Tae (1:2,000) (37), HA epitope (1:5,000), and ActC (1:5,000) (40), then incubated with horseradish peroxidase-conjugated anti-rabbit secondary antibody (1:20,000) and visualized with the ECL system (Perkin-Elmer).

Co-IP. Co-IP was performed as described previously (37) with modifications. Briefly, *A. tumefaciens* cells grown in 523 medium overnight were adjusted to OD_{600} 0.2 with I-medium (pH 5.5) and incubated at 25 °C with shaking. At 7-h postincubation, the cells equivalent to OD_{600} 5 per mL were harvested and subjected to DTBP cross-linking and were lysed in NP1 buffer (50 mM Tris·HCl pH 8.0, 0.5 M sucrose, 10 mM EDTA) containing 1 mM phenylmethylsulfonyl fluoride (PMSF) and 0.05% TritonX-100 by using a constant cell disruptor (Constant Systems). The cell lysates were centrifuged and the supernatant was collected as an input fraction. For co-IP, a 1.7-mL input fraction was incubated for 1 h with 10-mg Protein A-Sepharose beads (GE Healthcare) to remove nonspecifically binding proteins (precleaning). The precleaned input fraction was further incubated overnight with an appropriate antibody and 25-mg Protein A-Sepharose beads. The beads were washed five times with NP1 buffer containing 1 mM PMSF and 0.05% TritonX-100 and eluted by boiling at 96 °C in sample buffer for 10 min. For co-IP with anti-HA, the cross-linked cells were lysed in PBS buffer (pH 7.4) containing 1 mM PMSF and 0.05% TritonX-100 by using a constant cell disruptor. The ∼1.2-mL input fraction was incubated with monoclonal anti-HA agarose beads

(Sigma-Aldrich) overnight at 4 °C. The beads were washed five times with PBS buffer containing 1 mM PMSF and 0.05% TritonX-100 and eluted by boiling at 96 °C in sample buffer for 10 min. Proteins in the input and elute fractions were detected by Western blot analysis. The antibody specifically for VgrG1 co-IP, named α-VgrG1^{C}, was generated against VgrG1 epitope (789-INFKKGGPGESGSCLKSM-806) located at the C-terminal extension region. The antibody for Tde1 co-IP was obtained by passing the crude Tde1 antibody serum (used in Western blot analysis and generated by using two epitopes from Tde1: 245-EECKPEGGNDNSPD-258 and 264-NGTGKGDGNPDVPVS-278) through the 264-NGTGKGDGNPDVPVS-278 peptide coupled with Amino-Link Plus resin (Pierce).

ACKNOWLEDGMENTS. We thank the members of E.-M.L. laboratory for discussion and critically reading the manuscript; and the DNA Sequencing Core Laboratory at the Institute of Plant and Microbial Biology, Academia Sinica for technical support for DNA sequencing. Funding for this project was provided by the Institute of Plant and Microbial Biology, Academia Sinica (E.-M.L. and C.-H.K.); and Ministry of Science and Technology Grant MOST 104-2311-B-001-025-MY3 (to E.-M.L.).

1. Durand E, Cambillau C, Cascales E, Journet L (2014) VgrG, Tae, Tle, and beyond: The versatile arsenal of Type VI secretion effectors. *Trends Microbiol* 22(9):498–507.
2. Russell AB, et al. (2011) Type VI secretion delivers bacteriolytic effectors to target cells. *Nature* 475(7356):343–347.
3. English G, et al. (2012) New secreted toxins and immunity proteins encoded within the Type VI secretion system gene cluster of *Serratia marcescens*. *Mol Microbiol* 86(4):921–936.
4. Whitney JC, et al. (2013) Identification, structure, and function of a novel type VI secretion peptidoglycan glycoside hydrolase effector-immunity pair. *J Biol Chem* 288(37):26616–26624.
5. Altindis E, Dong T, Catalano C, Mekalanos J (2015) Secretome analysis of *Vibrio cholerae* type VI secretion system reveals a new effector-immunity pair. *MBio* 6(2):e00075.
6. Ma LS, Hachani A, Lin JS, Filloux A, Lai EM (2014) *Agrobacterium tumefaciens* deploys a superfamily of type VI secretion DNase effectors as weapons for interbacterial competition in planta. *Cell Host Microbe* 16(1):94–104.
7. Koskiniemi S, et al. (2013) Rhs proteins from diverse bacteria mediate intercellular competition. *Proc Natl Acad Sci USA* 110(17):7032–7037.
8. Alcoforado Diniz J, Coulthurst SJ (2015) Intraspecies competition in *Serratia marcescens* is mediated by type VI-secreted Rhs effectors and a conserved effector-associated accessory protein. *J Bacteriol* 197(14):2350–2360.
9. Dong TG, Ho BT, Yoder-Himes DR, Mekalanos JJ (2013) Identification of T6SS-dependent effector and immunity proteins by Tn-seq in *Vibrio cholerae*. *Proc Natl Acad Sci USA* 110(7):2623–2628.
10. Russell AB, et al. (2013) Diverse type VI secretion phospholipases are functionally plastic antibacterial effectors. *Nature* 496(7446):508–512.
11. Flaugnatti N, et al. (2016) A phospholipase A1 antibacterial type VI secretion effector interacts directly with the C-terminal domain of the VgrG spike protein for delivery. *Mol Microbiol* 99(6):1099–1118.
12. Chou S, et al. (2015) Transferred interbacterial antagonism genes augment eukaryotic innate immune function. *Nature* 518(7537):98–101.
13. Metcalf JA, Funkhouser-Jones LJ, Brileya K, Reysenbach AL, Bordenstein SR (2014) Antibacterial gene transfer across the tree of life. *eLife* 3:3.
14. Leiman PG, et al. (2009) Type VI secretion apparatus and phage tail-associated protein complexes share a common evolutionary origin. *Proc Natl Acad Sci USA* 106(11):4154–4159.
15. Basler M, Mekalanos JJ (2012) Type 6 secretion dynamics within and between bacterial cells. *Science* 337(6096):815.
16. Basler M, Pilhofer M, Henderson GP, Jensen GJ, Mekalanos JJ (2012) Type VI secretion requires a dynamic contractile phage tail-like structure. *Nature* 483(7388):182–186.
17. Kapitein N, et al. (2013) ClpV recycles VipA/VipB tubules and prevents non-productive tubule formation to ensure efficient type VI protein secretion. *Mol Microbiol* 87(5):1013–1028.
18. Brunet YR, Hénin J, Celia H, Cascales E (2014) Type VI secretion and bacteriophage tail tubes share a common assembly pathway. *EMBO Rep* 15(3):315–321.
19. Clemens DL, Ge P, Lee BY, Horwitz MA, Zhou ZH (2015) Atomic structure of T6SS reveals interlaced array essential to function. *Cell* 160(5):940–951.
20. Kudryashev M, et al. (2015) Structure of the type VI secretion system contractile sheath. *Cell* 160(5):952–962.
21. Durand E, et al. (2015) Biogenesis and structure of a type VI secretion membrane core complex. *Nature* 523(7562):555–560.
22. Zoued A, et al. (2016) Priming and polymerization of a bacterial contractile tail structure. *Nature* 531(7592):59–63.
23. Silverman JM, et al. (2013) Haemolysin coregulated protein is an exported receptor and chaperone of type VI secretion substrates. *Mol Cell* 51(5):584–593.
24. Blondel CJ, Jiménez JC, Contreras I, Santiviago CA (2009) Comparative genomic analysis uncovers 3 novel loci encoding type six secretion systems differentially distributed in *Salmonella* serotypes. *BMC Genomics* 10:354.
25. Pukatzki S, Ma AT, Revel AT, Sturtevant D, Mekalanos JJ (2007) Type VI secretion system translocates a phage tail spike-like protein into target cells where it cross-links actin. *Proc Natl Acad Sci USA* 104(39):15508–15513.
26. Suarez G, et al. (2010) A type VI secretion system effector protein, VgrG1, from *Aeromonas hydrophila* that induces host cell toxicity by ADP ribosylation of actin. *J Bacteriol* 192(1):155–168.
27. Brooks TM, Unterweger D, Bachmann V, Kostiuk B, Pukatzki S (2013) Lytic activity of the *Vibrio cholerae* type VI secretion toxin VgrG-3 is inhibited by the antitoxin TsaB. *J Biol Chem* 288(11):7618–7625.
28. Shneider MM, et al. (2013) PAAR-repeat proteins sharpen and diversify the type VI secretion system spike. *Nature* 500(7462):350–353.
29. Filloux A (2013) Microbiology: A weapon for bacterial warfare. *Nature* 500(7462):284–285.
30. Whitney JC, et al. (2014) Genetically distinct pathways guide effector export through the type VI secretion system. *Mol Microbiol* 92(3):529–542.
31. Hachani A, Allsopp LP, Oduko Y, Filloux A (2014) The VgrG proteins are "à la carte" delivery systems for bacterial type VI effectors. *J Biol Chem* 289(25):17872–17884.
32. Liang X, et al. (2015) Identification of divergent type VI secretion effectors using a conserved chaperone domain. *Proc Natl Acad Sci USA* 112(29):9106–9111.
33. Unterweger D, et al. (2015) Chimeric adaptor proteins translocate diverse type VI secretion system effectors in *Vibrio cholerae*. *EMBO J* 34(16):2198–2210.
34. Wu HY, Chung PC, Shih HW, Wen SR, Lai EM (2008) Secretome analysis uncovers an Hcp-family protein secreted via a type VI secretion system in *Agrobacterium tumefaciens*. *J Bacteriol* 190(8):2841–2850.
35. Wu CF, Lin JS, Shaw GC, Lai EM (2012) Acid-induced type VI secretion system is regulated by ExoR-ChvG/ChvI signaling cascade in *Agrobacterium tumefaciens*. *PLoS Pathog* 8(9):e1002938.
36. Lin JS, et al. (2014) Fha interaction with phosphothreonine of TssL activates type VI secretion in *Agrobacterium tumefaciens*. *PLoS Pathog* 10(3):e1003991.
37. Lin JS, Ma LS, Lai EM (2013) Systematic dissection of the agrobacterium type VI secretion system reveals machinery and secreted components for subcomplex formation. *PLoS One* 8(7):e67647.
38. Kelley LA, Sternberg MJ (2009) Protein structure prediction on the web: A case study using the Phyre server. *Nat Protoc* 4(3):363–371.
39. Marchler-Bauer A, Bryant SH (2004) CD-Search: protein domain annotations on the fly. *Nucleic Acids Res* 32(Web Server issue):W327–W331.
40. Liu AC, Shih HW, Hsu T, Lai EM (2008) A citrate-inducible gene, encoding a putative tricarboxylate transporter, is downregulated by the organic solvent DMSO in *Agrobacterium tumefaciens*. *J Appl Microbiol* 105(5):1372–1383.
41. Horton RM, Hunt HD, Ho SN, Pullen JK, Pease LR (1989) Engineering hybrid genes without the use of restriction enzymes: Gene splicing by overlap extension. *Gene* 77(1):61–68.
42. Comacho C, et al. (2009) Blast+: Architecture and applications. *BMC Bioinformatics* 10:421.
43. Benson DA, et al. (2015) GenBank. *Nucleic Acids Res* 43(Database issue):D30–D35.
44. Arnold K, Bordoli L, Kopp J, Schwede T (2006) The SWISS-MODEL workspace: A web-based environment for protein structure homology modelling. *Bioinformatics* 22(2):195–201.
45. Zhang Y (2008) I-TASSER server for protein 3D structure prediction. *BMC Bioinformatics* 9:40.
46. Lovell SC, et al. (2003) Structure validation by Calpha geometry: Phi, psi and Cbeta deviation. *Proteins* 50(3):437–450.
47. Wallner B, Elofsson A (2003) Can correct protein models be identified? *Protein Sci* 12(5):1073–1086.
48. Holm L, Rosenstrom P (2010) Dali server: Conservation mapping in 3D. *Nucleic Acids Res* 38(Web Server issue):W545–W549.
49. Schneider CA, Rasband WS, Eliceiri KW (2012) NIH Image to ImageJ: 25 years of image analysis. *Nat Methods* 9(7):671–675.